Attachment 3

WCAP-17385-NP, Revision 3 (Non-Proprietary)

Westinghouse Non-Proprietary Class 3

WCAP-17385-NP
Revision 3

May 2012

STP Unit 3 Steam Dryer Flow-Induced Vibration Assessment

Westinghouse

This page left intentionally blank.

WESTINGHOUSE NON-PROPRIETARY CLASS 3

WCAP-17385-NP
Revision 3

Robert D. Quinn*
ABWR Licensing

May 20122

Reviewer: Subhash Chandra*
ABWR Engineering and Operations

Approved: Nirmal K. Jain*, Manager
ABWR Engineering and Operations

*Electronically approved records are authenticated in the electronic document management system.

Westinghouse Electric Company LLC
1000 Westinghouse Drive
Cranberry Township, PA 16066

© 2012 Westinghouse Electric Company LLC
All Rights Reserved

This page left intentionally blank.

TABLE OF CONTENTS

1 INTRODUCTION 1-1
1.1 BACKGROUND 1-1
1.2 APPROACH - OVERVIEW 1-1
1.3 REFERENCES FOR SECTION 1 1-5

2 STEAM DRYER DESCRIPTION 2-1
2.1 REFERENCES FOR SECTION 2 2-4

3 ABWR OPERATING EXPERIENCE 3-1
3.1 OPERATING EXPERIENCE 3-1
3.2 REFERENCES FOR SECTION 3 3-5

4 ELIMINATION OF ACOUSTIC RESONANCE 4-1
4.1 DESIGN MODIFICATION 4-1
4.2 SUBSCALE TEST 4-2
4.3 REFERENCES FOR SECTION 4 4-4

5 DRYER STARTUP INSTRUMENTATION AND STRUCTURAL EVALUATION 5-1
5.1 FINITE ELEMENT MODEL 5-2
5.1.1 Modal Analysis 5-13
5.2 DRYER INSTRUMENTATION METHODOLOGY 5-15
5.2.1 Methodology 5-15
5.2.2 [ ]a,c 5-15
5.2.3 Application to Strain Gage Measurements 5-19
5.2.4 Numerical Implementation Details 5-20
5.2.5 Stress Evaluation for Instrumentation 5-32
5.2.6 Application of Frequency Shifting and Biases and Uncertainties 5-33
5.3 DRYER INSTRUMENTATION 5-35
5.3.1 Pressure Transducers 5-35
5.3.2 SG Locations 5-41
5.3.3 Accelerometer 5-48
5.4 RESULTS OF INSTRUMENTATION EVALUATION 5-49
5.4.1 Condition Number and Rank for PT Arrangement 5-49
5.4.2 Condition Number and Rank for SG Arrangement 5-53
5.5 STRUCTURAL EVALUATION USING RJ-ABWR STARTUP DATA 5-55
5.5.1 Structural Evaluation Overview 5-55
5.5.2 Methodology 5-56
MSL Acoustic 5-77
5.5.3 Structural Analysis 5-77
5.5.4 Non-MSL Acoustic Loads 5-81
5.5.5 Results 5-88
5.6 SUMMARY 5-121
5.7 REFERENCES FOR SECTION 5 5-122

6 STEAM DRYER POWER ASCENSION PLAN 6-1
6.1 APPROACH - OVERVIEW 6-1
6.2 LIMIT CURVE METHODOLOGY 6-2
6.3 POWER ASCENSION PROCESS 6-4
6.4 VALIDATION OF THE USE OF [ ][a,c] 6-6
6.5 BIASES AND UNCERTAINTIES 6-13
6.5.1 Bias and Uncertainty at [ ][a,c] Power 6-13
6.6 REFERENCES FOR SECTION 6 6-20

7 CONCLUSIONS 7-1
7.1 REFERENCES FOR SECTION 7 7-3

LIST OF TABLES

Table 3.1-1 Comparison of STP Dryer with Other BWR/2-6 Dryers 3-2

Table 3.1-2 [ ]^{a,c} 3-3

Table 3.1-3 [ ]^{a,c} 3-4

Table 5.1-1 Comparison of RJ-ABWR Hammer Test and STP Modal Analysis Results 5-14

Table 5.3.1-1 PT Locations 5-37

Table 5.3.2-1 Strain Gage Locations 5-43

Table 5.3.3-1 Accelerometer Locations 5-48

Table 5.4.1-1 Condition Numbers and Frequency for PT Sensor Arrangement 1 5-50

Table 5.4.2-1 Condition Numbers and Frequency for SG Sensor Arrangement 5-53

Table 5.5.2.1-1 Applicable RJ-ABWR Steam DryerMeasurement Descriptions and Locations 5-57

Table 5.5.2.1-2 [ ]^{a,c} 5-68

Table 5.5.3.4-1 Maximum Allowable Stress Intensities and Alternating Stress Endurance Limit 5-80

Table 5.5.4.3-1 p-p Values from Sensor Time Histories 5-84

Table 5.5.4.3-2 [ ]^{a,c} 5-86

Table 5.5.5.1-1 Locations with Highest Predicted Stress at 100% Power 5-90

Table 5.5.5.2-1 Limiting Non-weld Locations with at 100% Power Operating Condition 5-97

Table 5.5.5.2-2 Limiting Peak Stress Ratios, SR-P, on Welds at 100% Power Operating Condition 5-98

Table 5.5.5.2-3 Limiting Alternating Stress Ratios, SR-a, on Welds at 100% Power Operating Condition 5-99

Table 6.5-1 Bias and Uncertainty for [ ]^{a,c} 6-15

This page left intentionally blank.

LIST OF FIGURES

Figure 2-1 ABWR Reactor Internal Component Arrangement 2-2
Figure 2-2 Steam Dryer 2-3
Figure 4.1-1 Modified Stand Pipe Design 4-1
Figure 4.2-1 [ ]a,c 4-3
Figure 5.1-1 Steam Dryer FEM 5-5
Figure 5.1-2 [ ]a,c 5-6
Figure 5.1-3 [ ]a,c 5-7
Figure 5.1-4 Vane Bank [ ]a,c 5-7
Figure 5.1-5 Vane Bank Mass Blocks 5-8
Figure 5.1-6 [ ]a,c 5-8
Figure 5.1-7 Hood Supports 5-9
Figure 5.1-8 Hoods 5-9
Figure 5.1-9 Dryer Viewed From Below 5-10
Figure 5.1-10 Skirt and Drain Ducts 5-10
Figure 5.1-11 Lifting Rods 5-11
Figure 5.1-12 Moment Transfer Beams 5-11
Figure 5.1-13 Vane Bank Details 5-12
Figure 5.1-14 Solid Element Vane Bank Mass Blocks 5-13
Figure 5.2.2-1 Steam Dryer Schematic with One MSL Entrance 5-16
Figure 5.2.2-2 [ ]a,c 5-16
Figure 5.2.4-1(a) [ ]a,c 5-22
Figure 5.2.4-1(b) [ ]a,c 5-23
Figure 5.2.4-2(a) [ ]a,c 5-24
Figure 5.2.4-2(b) [ ]a,c 5-25
Figure 5.2.4-3(a) [ ]a,c 5-26

Figure 5.2.4-3(b) [ ]a,c 5-27

Figure 5.2.4-4(a) [ ]a,c 5-28

Figure 5.2.4-4(b) [ ]a,c 5-29

Figure 5.2.4-5(a) [ ]a,c 5-30

Figure 5.2.4-5(b) [ ]a,c 5-31

Figure 5.3.1-1 RJ-ABWR Steam Dryer Instrumentation 5-38

Figure 5.3.1-2 PT Locations [ ]a,c 5-39

Figure 5.3.1-3 PT Locations [ ]a,c 5-40

Figure 5.3.2-1 [ ]a,c 5-44

Figure 5.3.2-2 [ ]a,c 5-45

Figure 5.3.2-3 Strain Gage Locations [ ]a,c 5-46

Figure 5.3.2-4 Strain Gage Locations [ ]a,c 5-47

Figure 5.3.3-1 Accelerometer Locations 5-48

Figure 5.4.1-1 Condition Number Variation with Frequency for PT Sensor Arrangement 1 5-51

Figure 5.4.1-2 Rank Calculated in SGELSS using RCOND=0.01 5-52

Figure 5.4.2-1 Condition Number Variation with Frequency for SG Sensor Arrangement 5-54

Figure 5.5.2.1-1 [ ]a,c 5-58

Figure 5.5.2.1-2 Comparison of Acceleration Data Collected on RJ-ABWR with Model Predictions for the A1 Accelerometer 5-61

Figure 5.5.2.1-3 Comparison of Displacement Data Collected on RJ-ABWR with Model Predictions for the A2 Accelerometer 5-61

Figure 5.5.2.1-4 Comparison of Displacement Data Collected on RJ-ABWR with Model Predictions for the A3 Accelerometer 5-62

Figure 5.5.2.1-5 Comparison of Displacement Data Collected on RJ-ABWR with Model Predictions for the A4 Accelerometer 5-62

Figure 5.5.2.1-6 Comparison of Strain Data Collected on RJ-ABWR with Model Predictions for the S1 Strain Gage 5-63

Figure 5.5.2.1-7 Comparison of Strain Data Collected on RJ-ABWR with Model Predictions for the S2 Strain Gage 5-63

Figure 5.5.2.1-8 Comparison of Strain Data Collected on RJ-ABWR with Model Predictions for the S3 Strain Gage 5-64

Figure 5.5.2.1-9 Comparison of Strain Data Collected on RJ-ABWR with Model Predictions for the S4 Strain Gage 5-64

Figure 5.5.2.1-10 Comparison of Strain Data Collected on RJ-ABWR with Model Predictions for the S5 Strain Gage 5-65

Figure 5.5.2.1-11 Comparison of Strain Data Collected on RJ-ABWR with Model Predictions for the S6 Strain Gage 5-65

Figure 5.5.2.1-12 Comparison of Strain Data Collected on RJ-ABWR with Model Predictions for the S7 Strain Gage 5-66

Figure 5.5.2.1-13 Comparison of Strain Data Collected on RJ-ABWR with Model Predictions for the P3 Pressure Transducer 5-66

Figure 5.5.2.1-14 Comparison of Strain Data Collected on RJ-ABWR with Model Predictions for the P4 Pressure Transducer 5-67

Figure 5.5.2.1-15 Comparison of Strain Data Collected on RJ-ABWR with Model Predictions for the P5 Pressure Transducer 5-67

Figure 5.5.2.1-16 Predicted MSL Entrance Source Pressures - PSD 5-68

Figure 5.5.2.5-1(a) [ ]a,c 5-74

Figure 5.5.2.5-1(b) [ ]a,c 5-75

Figure 5.5.2.5-1(c) [ ]a,c 5-76

Figure 5.5.3.1-1 [ ]a,c 5-78

Figure 5.5.4.3-1 Skirt, Drain Channel, and Support Ring Model With Discrete Supports at Four Support Lugs 5-87

Figure 5.5.5.1-1 [ ]a,c 5-91

Figure 5.5.5.1-2 [ ]a,c 5-92

Figure 5.5.5.1-3 [ ]a,c 5-93

Figure 5.5.5.1-4 [ ]a,c 5-94

Figure 5.5.5.1-5 [ ]a,c 5-95

Figure 5.5.5.2-1 Locations of Limiting Peak Stress Ratios, [ ]^{a,c}, at Non-Welds – Location 1 .5-100

Figure 5.5.5.2-2 Locations of Limiting Peak Stress Ratios, [ ]^{a,c}, at Non-Welds – Locations 2 and 3 5-101

Figure 5.5.5.2-3 Locations of Limiting Alternating Stress Ratios, [ ]^{a,c}, at Non-Welds – Locations 1-5 5-102

Figure 5.5.5.2-4 Locations of Limiting Alternating Stress Ratios, [ ]^{a,c}, at Non-Welds 5-103

Figure 5.5.5.2-5 Locations of Limiting Stress Ratios, [ ]^{a,c}, at Welds....5-104

Figure 5.5.5.2-6 Locations of Limiting Stress Ratios, [ ]^{a,c}, at Welds....5-105

Figure 5.5.5.2-7 Locations of Limiting Stress Ratios, [ ]^{a,c}, at Welds....5-106

Figure 5.5.5.2-8 Locations of Limiting Alternating Stress Ratios, [ ]^{a,c}, at Welds 5-107

Figure 5.5.5.2-9 Locations of Limiting Alternating Stress Ratios, [ ]^{a,c}, at Welds 5-108

Figure 5.5.5.2-10 Locations of Limiting Alternating Stress Ratios, [ ]^{a,c}, at Welds 5-109

Figure 5.5.5.3-1 Accumulative PSD and PSD Curves of the σ_{yy} Stress Response at Node 128691; Dominant Frequency: 59.5 Hz....5-112

Figure 5.5.5.3-2 Accumulative PSD and PSD of the σ_{zx} Stress Response at Node 103032; Dominant Frequency: 95.1 Hz....5-113

Figure 5.5.5.3-3 Accumulative PSD and PSD of the σ_{xx} Stress Response at Node 83569; Dominant Frequency: 15.1 Hz....5-114

Figure 5.5.5.3-4 Accumulative PSD and PSD of the σ_{zz} Stress Response at Node 3053; Dominant Frequency: 20.1 Hz....5-115

Figure 5.5.5.3-5 Accumulative PSD and PSD of the σ_{zz} Stress Response at Node 84160; Dominant Frequency: 15.1 Hz....5-116

Figure 5.5.5.3-6 Accumulative PSD and PSD of the σ_{zz} Stress Response at Node 102649; Dominant Frequency: 18.0 Hz....5-117

Figure 5.5.5.3-7 Contour Map Showing the Dominant Frequencies (0-25 Hz)....5-118

Figure 5.5.5.3-8 Contour Map Showing the Dominant Frequencies (25-75 Hz)....5-119

Figure 5.5.5.3-9 Contour Map Showing the Dominant Frequencies (75-200 Hz)....5-120

Figure 6.2-1 Schematic of the Solution Field 6-2

Figure 6.4-1 Schematic of the Subscale PT Locations IDP1 to IDP12 (Reference 6-5) 6-7

Figure 6.4-2 Schematic of the [ ]^{a,c}....6-8

Figure 6.4-3 [ ]^{a,c} 6-9

Figure 6.4-4 [

]a,c 6-10

Figure 6.4-5 [

]a,c 6-11

Figure 6.4-6 [

]a,c 6-12

Figure 6.5-1 [

]a,c 6-16

Figure 6.5-2 [

]a,c 6-17

Figure 6.5-3 [

]a,c 6-18

Figure 6.5-4 [

]a,c 6-19

LIST OF ACRONYMS

ABWR	Advanced Boiling Water Reactor
ACM	Acoustic Circuit Model
ASB	Acoustic Side Branch
ASME	American Society of Mechanical Engineers
BWR	Boiling Water Reactor
BWRVIP	Boiling Water Reactor Vessel Internals Program
CRD	Control Rod Drive
CRGT	Control Rod Guide Tube
CVAP	Comprehensive Vibration Assessment Program
DCD	Design Control Document
DP	Dipole
DPh	Unit dipole in the horizontal direction
DPv	Unit dipole in the vertical direction
EPU	Extended Power Uprate
ERV	Electromatic Relief Valve
FE	Finite Element
FEA	Finite Element Analysis
FEM	Finite Element Model
FFT	Fast Fourier Transform
FIV	Flow-Induced Vibration
FW	Feedwater
HPCF	High Pressure Core Flooder
ICMGT	In-Core Monitor Guide Tube
ICM	In-Core Monitor
IGSCC	Intergranular Stress Corrosion Cracking
J-ABWR	Japanese ABWR
LPFL	Low Pressure Flooder
LSR	Lower Support Ring
MP	Monopole
MSIV	Main Steam Isolation Valve
MSL	Main Steam Line
NDE	Nondestructive Examination
NRC	U.S. Nuclear Regulatory Commission
OLTP	Original Licensed Thermal Power
PORV	Pilot Operated Relief Valve
PSD	Power Spectral Density
PT	Pressure Transducer
RG	Regulatory Guide
RIP	Reactor Internal Pump
RJ-ABWR	Reference Japanese ABWR
RPV	Reactor Pressure Vessel
RMS	Root Mean Square

SCF	Stress Concentration Factor
SG	Strain Gage
SMT	Scale Model Test
SRSS	Square-Root-Sum-of-the-Squares
SRV	Safety Relief Valve
STP	South Texas Project
TSVC	Turbine Stop Valve Closure
USR	Upper Support Ring

ANSYS, ANSYS Workbench, AUTODYN, CFX, FLUENT and any and all ANSYS, Inc. brand, product, service and feature names, logos and slogans are registered trademarks or trademarks of ANSYS, Inc. or its subsidiaries in the United States or other countries. [ICEM CFD is a trademark used by ANSYS, Inc. under license.]* All other brand, product, service and feature names or trademarks are the property of their respective owners.

EXECUTIVE SUMMARY

The South Texas Project Unit 3 (STP Unit 3) nuclear power plant is the first Advanced Boiling Water Reactor (ABWR) constructed in the U.S. ABWRs have been successfully operating since 1996 in Japan; there are four similar ABWRs currently operating in Japan and two more units are under construction in Japan. In addition, two other ABWRs are under construction in Taiwan.

U.S. NRC Regulatory Guide (RG) 1.20, Comprehensive Vibration Assessment Program for Reactor Internals during Preoperational and Initial Startup Testing, provides guidance for the comprehensive vibration assessment program (CVAP) for nuclear power plants during preoperational and initial startup testing. The program is intended to demonstrate that the reactor internals are adequately designed to withstand flow-induced vibration (FIV) forces at normal and transient plant operating conditions for the design life of the plant. The latest revision (Revision 3, March 2007) of RG 1.20 contains additional requirements based with recent Boiling Water Reactor (BWR) experiences on the steam dryers. STP Unit 3 is designated as a prototype plant. Kashiwazaki-Kariwa Unit 6, herein referred to as the reference Japanese ABWR (RJ-ABWR), commenced successful commercial operation in 1996 and went through extensive testing to show that the reactor internals are adequately designed to withstand FIV loads.

This report documents the approach used to qualify the STP Unit 3 steam dryer for FIV loads using the guidance of RG 1.20, Revision 3. The structural qualification of the STP Unit 3 steam dryer is based on the following considerations:

Operating Experience

The STP dryers are essentially identical to the RJ-ABWR and [ ]^{a,c}, herein referred to as the J-ABWR. The RJ-ABWR has operated for over twelve years and the J-ABWR has operated since 2005. The operating ABWRs have dryers that are essentially identical in both configuration and plant operating conditions. The dryers for both operating plants have been inspected and no indications have been found. In addition, the ABWR dryer incorporates improvements in the dryer design that results in greater structural capability and better performance than earlier dryer designs.

Design Modifications to Avoid Acoustic Resonance

Subscale testing was performed to determine if an acoustic resonance would occur for power levels up to 100%. The initial subscale tests [

]^{a,c} Although the operating experience and inspection results [

]^{a,c} Additional subscale testing was performed to [
]^{a,c}

Instrumentation During Startup

The STP Unit 3 steam dryer will be instrumented and monitored during initial plant startup with pressure transducers, strain gages, and accelerometers. To ensure that the operating experience for the dryer stresses are below the fatigue endurance limit, a confirmatory plan to hold the plant during initial startup

at 60% power to generate limit curves will be performed. Data will be collected at increments of [ ]^{a,c} power up to 100% and limit curves will be generated at each [ ]^{a,c} power increment.

Structural Evaluation Using RJ-ABWR Data

While the primary basis for qualification of the STP steam dryer is operating experience, a structural evaluation of the STP steam dryer was performed using RJ-ABWR startup data. The results of this structural evaluation showed that the dryer stresses were below the allowable limit of 9.95 ksi (68.6 MPa).

Thus, the [

]^{a,c} will ensure the structural adequacy of the STP steam dryer to withstand FIV loads.

This page left intentionally blank.

1 INTRODUCTION

1.1 BACKGROUND

The main function of the steam dryer in a Boiling Water Reactor (BWR) is to remove moisture from the steam in order to minimize erosion of piping and the turbine. The dryer is not safety-related and is not an ASME Code component. Although there have been some differences in the design configuration of the steam dryer with evolution of BWR types (BWR/2-6) and the Advanced Boiling Water Reactor (ABWR), the basic features of the dryer have remained essentially the same.

The steam dryer assembly is mounted in the reactor vessel above the separator assembly and forms the top and sides of the wet steam plenum. During refueling operations, the dryer is removed to allow access to the reactor core. Vertical guide rods on the inside of the vessel provide alignment for the dryer assembly during re-installation. The dryer assembly is supported by brackets extending inward from the vessel wall and is held down in position during operation by the vessel head hold down brackets. Steam from the separators flows upward and outward through the dryer's drying vanes. These vanes are attached to a top and bottom supporting member forming a rigid integral unit. Moisture is removed and carried by a system of troughs and drains to the pool surrounding the separators and then into the recirculation downcomer annulus between the core shroud and reactor vessel wall.

Regulatory Guide (RG) 1.20 provides guidance for the comprehensive vibration assessment program (CVAP) for nuclear power plants during preoperational and initial startup testing. The program is intended to demonstrate that the reactor internals are adequately designed to withstand flow-induced vibration (FIV) forces at normal and transient plant operating conditions for the design life of the plant. The ABWR was designed and certified under RG 1.20 Revision 2. This same design is employed in multiple ABWR plants in Japan. One of those Japanese ABWRs, as described in WCAP-17370-P (Reference 1-2) and referred to as the reference Japanese ABWR (RJ-ABWR), commenced commercial operation in 1996 after going through extensive preoperational and start-up testing to confirm that the reactor internals are adequately designed to withstand FIV loads. The RJ-ABWR steam dryer has an excellent operating history as demonstrated by tests and inspections. The latest revision (Revision 3, March 2007) of RG 1.20 contains additional requirements based on recent BWR experiences on steam dryers. Based on the need to address the current guidance, STPNOC (now NINA) decided that STP Unit 3 reactor internals will be designated as the U.S. ABWR prototype.

1.2 APPROACH - OVERVIEW

As stated above, the steam dryer design in the ABWR certified design was developed to satisfy the guidance of RG 1.20 Revision 2. The Final Safety Evaluation Report (FSER) for the ABWR (NUREG-1503) states that the response of the dryer to FIV must be predicted before final design approval; discusses the analyses that were done by the Design Certification (DC) applicant which were reviewed by the Nuclear Regulatory Commission (NRC) staff; and concludes that the combination of predictive analysis, pre-test inspections, tests, and post-test inspections assures that the reactor internals will perform without loss of structural integrity. The DCD specifies a peak stress amplitude limit that is significantly lower than the ASME Code allowable value (the ASME allowable is approximately 37% higher than the DCD allowable value). Thus, the certified dryer design has a predictive analysis that is adequate for this lower allowable stress. This has been confirmed by pre-operational testing at the RJ-ABWR, which

confirmed the peak and alternating stresses in the steam dryer meet the allowable limit, and that the maximum stresses are less than this conservative allowable limit.

RG 1.20 Revision 3 Part D – Implementation, states, "Except in those cases in which a licensee proposes or has previously established an acceptable alternative method for complying with specified portions of the NRC's regulations, the NRC staff will use the methods described in this guide…" . Because the certified ABWR steam dryer design was not designed specifically to meet the guidance of RG 1.20 Revision 3 (as portions of this guidance were not available at the time), but was designed to satisfy the earlier guidance of RG 1.20 Revision 2, the approach to show the structural acceptability of the dryer is to use a combination of the previously established qualification of the dryer along with a proposed alternative to provide a means to demonstrate that the reactor internals will perform without loss of structural integrity, as discussed in the FSER. The alternate approach consists of the activities as described in the following paragraphs:

Operating Experience

[

]a,c

Eliminate Acoustic Resonance

To ensure that the STP steam dryer is not subjected to acoustic loads, subscale tests were performed to confirm that the design of the safety relief valve (SRV) branch connections and stand pipe do not generate acoustic loads on the dryer. Modifications to the [ ]a,c were tested to ensure that acoustic resonance will not occur at power levels up to 100%.

Dryer Instrumentation During Startup

The STP Unit 3 dryer instrumentation uses an approach that utilizes a [ ]a,c and relies on the [ ]a,c to determine associated stress response due to a [ ]a,c that is used to determine locations. It also locates instruments to confirm the load definition and measure the steady state operating stresses. The [ ]a,c refers to the acoustic field in the steam dome and the associated stress response resulting when imposing a [ ]a,c at one of the main steam line (MSL) entrances while setting the [ ]a,c Each solution is calculated numerically by solving the Helmholtz equation in the steam dome for the given acoustic sources and calculating the stress response on the steam dryer resulting from this acoustic load. Dryer locations that show [ ]a,c are used to determine the sensor types and locations.

Structural Evaluation Using RJ-ABWR Data

While the main basis for qualification of the STP steam dryer is operating experience, a structural evaluation of the STP steam dryer was performed using RJ-ABWR startup data. The results of this structural evaluation showed that the dryer stresses were below the allowable limit of 9.95 ksi (68.6 MPa).

Startup Test – Power Ascension Plan

Additionally, the startup testing will include an initial hold point at 60% power to collect steam dryer data and generate limit curves to ensure that the steam dryer stresses are below the fatigue limit. Thereafter, for every [ ]^{a,c} power increment up to [ ]^{a,c} power, the plant will hold power to collect steam dryer data and generate limit curves.

To ensure that the dryer stresses are within acceptable limits, the following steps will be taken during power ascension:

1. Power will be held at approximately 60% power so that dryer instrumentation data can be collected and the minimum stress ratio will be computed. Two sets of limit curves will be generated for continuing power ascension based on selected pressure transducers on the STP Unit 3 steam dryer. The limit curves stress level are predicted on the full scale STP steam dryer and represent the accelerometer, strain gage, and/or pressure transducer locations or combinations of locations. The limit curves will be provided to the NRC for information only.

   Measurements at a minimum of [ ]^{a,c} pressure transducer locations will be required during power ascension so that monopole and dipole sources can be computed at each of the four MSL entrances. The MSLs will be instrumented with strain gages for [ ]^{a,c}. MSL data [ ]^{a,c} steam dryer qualification.

2. Power ascension will continue to [ ]^{a,c} power and the limit curves will be redrawn. If the limit curves are not exceeded, power ascension will continue and the revised limit curves will be supplied to the NRC for information only. If the limit curves are exceeded, the procedure discussed below will be followed.

3. Power ascension will continue to [ ]^{a,c} power and the limit curves will be redrawn. If the limit curves are not exceeded, power ascension will continue and the revised limit curves will be supplied to the NRC for information only. If the limit curves are exceeded, the procedure discussed below will be followed.

4. Power ascension will continue to [ ]^{a,c} power and the limit curves will be redrawn. If the limit curves are not exceeded, power ascension will continue, and the revised limit curves will be supplied to the NRC for information only. If the limit curves are exceeded, the procedure discussed below will be followed.

5. Power ascension will continue to 100% power and the limit curves will be redrawn. A full stress report will then be prepared and submitted to the NRC for review and approval per RG 1.20 Revision 3 (Reference 1-1).

At the power levels defined above, accelerations, strains, and pressures will be recorded at selected locations on the STP Unit 3 steam dryer and the procedure described below will be followed to be consistent with the approach implemented previously for other BWR steam dryers. [

]^{a,c}

During power ascension, should any of these quantities exceed a Level 2 limit curve, the power will be held at that power level until a real-time stress analysis is performed to develop new limit curves. Should a Level 1 limit curve be exceeded, the power will be reduced to a previous power level in which Level 1 was not exceeded and a real-time stress analysis will be performed to develop new limit curves.

Thus, the [

]^{a,c} will ensure the structural adequacy of the STP steam dryer to withstand FIV loads.

Section 2 provides an overview of the dryer design.

Section 3 discusses the operating experience of ABWRs. Specifically addressed is the field experience that led to improvements in the ABWR dryer design, and the successful operation and available inspection of [ ]^{a,c} ABWRs in Japan.

Section 4 describes the [ ]^{a,c} performed to [ ]^{a,c} acoustic resonance in the ABWR.

Section 5 describes the dryer instrumentation used during initial startup of STP Unit 3 and the structural evaluation of the dryer using RJ-ABWR startup data. This includes the methodology used to determine the sensor types, number of sensors, and sensor locations.

Section 6 discusses the steam dryer power ascension plan, including the methodology for generation of the limit curves, the application of the biases and uncertainties, as appropriate, and the validation of using pressure data at select locations develop loads for the rest of the dryer.

Section 7 summarizes the technical basis for the conclusion that the STP Unit 3 dryer is structurally adequate to withstand FIV loads.

1.3 REFERENCES FOR SECTION 1

1-1 U.S. NRC Regulatory Guide 1.20, Rev. 3, "Comprehensive Vibration Assessment Program for Reactor Internals during Preoperational and Initial Startup Testing," March 2007.

1-2 Westinghouse Report, WCAP-17370-P, Rev. 3 "South Texas Project Unit 3 Comprehensive Vibration Assessment Program, Measurement, Test and Inspection Plan," May 2012. (Proprietary)

This page left intentionally blank.

2 STEAM DRYER DESCRIPTION

The STP Unit 3 reactor internal components are shown in Figure 2-1. The steam dryer is located in the steam dome. Figure 2-1 shows the location of the steam dryer relative to the rest of the reactor internal components.

The steam dryer consists of an upper and lower assembly. The upper assembly consists of the dryer banks, hoods, and troughs. The lower assembly includes the skirt and the drain channels. The upper and lower assemblies are connected by a support ring. The steam dryer is supported by four brackets welded on the vessel shell at the location of the support ring. Figure 2-2 shows the steam dryer and the steam dryer components.

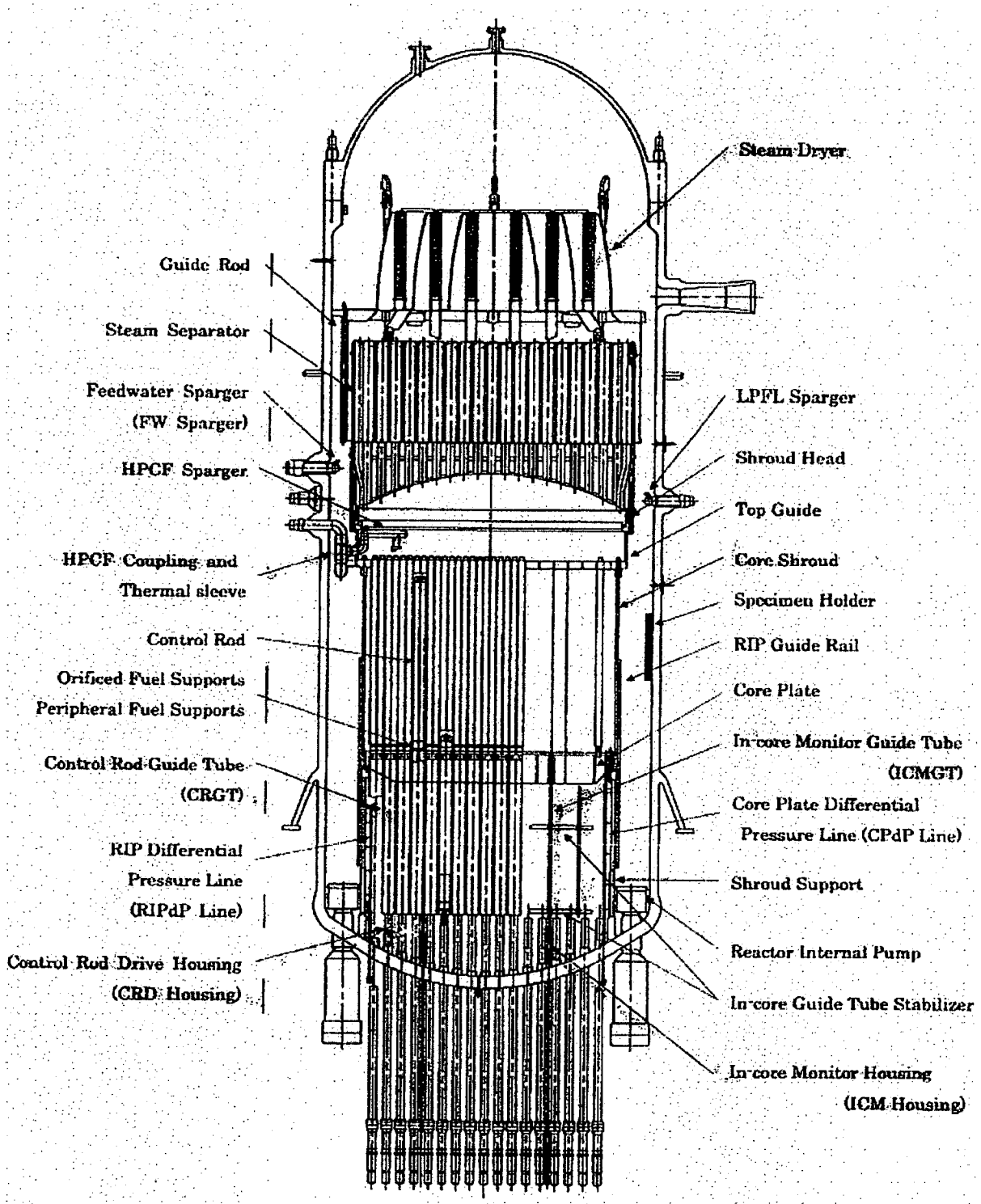

Figure 2-1 ABWR Reactor Internal Component Arrangement (Taken from Reference 2-1)

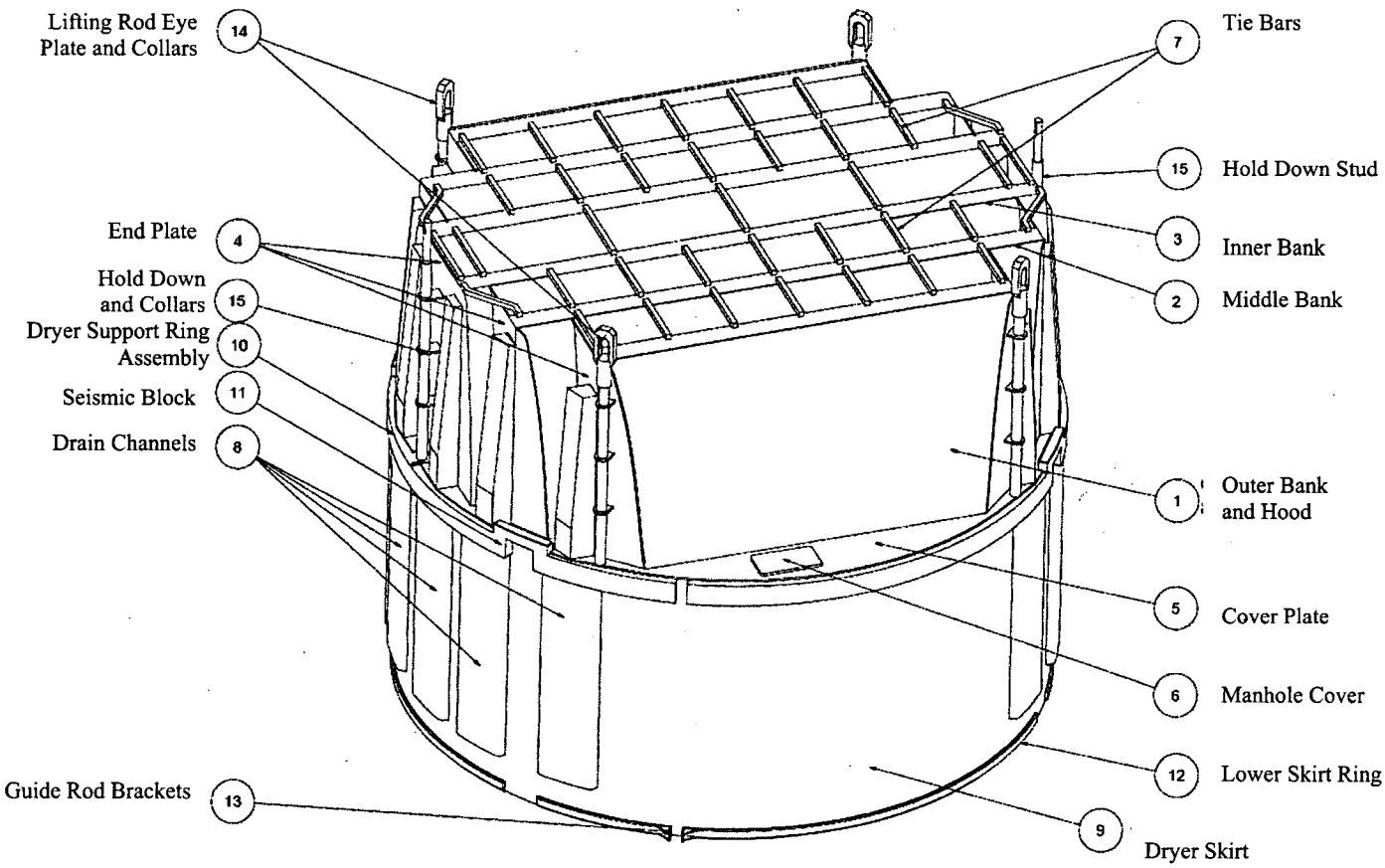

Figure 2-2 Steam Dryer

2.1 REFERENCES FOR SECTION 2

2-1 Toshiba Document, RS-5126954, Rev. 1, "Prototype ABWR Reactor Internals Flow Induced Vibration Test Report." (Proprietary)

3 ABWR OPERATING EXPERIENCE

The ABWR is an evolutionary design that builds on operating BWR experience and includes significant design improvements in the dryer design.

3.1 OPERATING EXPERIENCE

Historically, there have been instances of minor cracking in BWR steam dryers, with the exception of the more significant Quad Cities Extended Power Uprate (EPU)-related dryer cracking. A variety of options, (e.g., hole drilling to stop crack growth, increasing weld size, and replacement of plates with thicker plates), have been implemented successfully as design fixes. Cracking in the dryer would have to be very significant to cause structural integrity concerns. Because dryers are visually inspected after removal in outages, significant cracking and associated loose parts due to cracking during the subsequent cycle are unlikely (the experience at the two Quad Cities units was an exception because of the Electromatic Relief Valve (ERV) stand pipe configuration that caused acoustic resonance and subsequent dryer cracks when EPU conditions were applied. When cracking has occurred as a result of plant operation, design fixes were implemented successfully and subsequent designs (such as the RJ-ABWR) incorporated the design fix ideas applied to the previous dryer designs. The successful operating experience with the RJ-ABWR and J-ABWR dryers (which are essentially identical to the STP dryers) shows that the design improvements based on the fixes for previous steam dryer problems have been effective. Table 3.1-1 shows a summary of the improvements to those ABWR dryers.

Reference 3-1 documents the successful operating experience and results of inspections of [ ]^{a,c} operating ABWRs. [

]^{a,c}

In 2007, RJ-ABWR experienced an earthquake that exceeded the original seismic design and the plant was shutdown for inspections and evaluations. [

]^{a,c}

[ ]^{a,c}

Table 3.1-1 Comparison of STP Dryer with Other BWR/2-6 Dryers

a,b,c

Cracking Attribute			
Component	Support Ring		
	Drain Channel		
	Dryer Hood		
	Tie Bar		
	Skirt		
	Lifting Rod		
Cracking Mechanism	IGSCC		
	Fatigue		
	Crevice cracking		
	Acoustic Resonance		
Regulatory Codes	ASME		
	BWRVIP		

Table 3.1-2 [ ][a,c]

[ ] a,b,c

Table 3.1-3 [**]**[a, c]

[ ]a,b,c

3.2 REFERENCES FOR SECTION 3

3-1 Westinghouse Report, WCAP-17369-P, "ABWR Dryer Operating Experience for STP Units 3 and 4," February 2011. (Proprietary)

This page left intentionally blank.

4 ELIMINATION OF ACOUSTIC RESONANCE

Startup data for the RJ-ABWR shows that the [ ]a,c Even though [ ]a,c on the RJ-ABWR and J-ABWR dryers. Although there is an [ ]a,c have been performed on the RJ-ABWR and J-ABWR dryers, the [ ]a,c has been [ ]a,c

Thus, the [ ]a,c and subscale tests were performed to confirm that no resonance occurs up to 100% power level.

4.1 DESIGN MODIFICATION

[a,c]

Figure 4.1-1 Modified Stand Pipe Design

4.2 SUBSCALE TEST

Subscale tests were performed for STP Unit 3; the initial test loop consisted of a four loop acoustic test model as described in the test plan (Reference 4-2) and documented in Reference 4-3. The four loop acoustic test model includes the reactor and plant from the steam-water interface in the reactor pressure vessel (RPV) to the pressure equalizer just upstream of the turbine, the four MSLs, and the SRVs. Figure 4.2-1 shows a photograph of the four loop test setup. Details of the development of the design of the four loop acoustic test model are documented in Reference 4-4.

The four loop subscale test had [

]a,c

The [ ]a,c described in Section 4.1 was tested in a [

]a,c

Tests were performed that corresponded to plant operation at [
]a,c configurations. The RJ-ABWR configuration was initially tested on the single loop test setup to confirm that the test setup resulted in the same results as the four loop configuration.

Subscale Test Results

Tests on the four loop setup were performed at a range of power levels for this configuration from [
]a,c plant power levels (Reference 4-6). The [
]a,c in the four loop tests. The RJ-ABWR SRV [

]a,c

The [ ]a,c and a single line subscale test was performed to confirm that acoustic resonance will not occur for operating conditions up to 100% power. The results of the [
]a,c showed that acoustic resonance does not occur for power levels up to 110% (Reference 4-5). [

]a,c Details of the single line test results are documented in Reference 4-5.

Note that the models for the subscale test [

]a,c

Conclusion

The modification to the [ ]a,c will eliminate the acoustic resonance for STP Units 3 and 4.

a,c

Figure 4.2-1 [ ][a,c]

4.3 REFERENCES FOR SECTION 4

4-1 Fauske and Associates Report, FAI/10-587, Rev. 0, "South Texas Unit 3 Single Line Acoustic Model Test Specification," January 2011. (Proprietary)

4-2 Fauske and Associates Report, FAI/10-445 Rev. 0, "South Texas Unit 3 Supplemental Test Plan for 4 Loop Acoustic Model," October 2010. (Proprietary)

4-3 Fauske and Associates Report, FAI/10-547, Rev. 0, "South Texas (STP) Unit 3 Supplemental Test Report for 4 Loop Acoustic Model – Data Evaluation," November 2010. (Proprietary)

4-4 Westinghouse Report, CN-A&SA-10-31, Rev. 1, "South Texas Unit 3 Scaling to Four Line Subscale Model," July 2010. (Proprietary)

4-5 Fauske and Associates Report, FAI/11-0105, Rev. 0, "South Texas Project (STP) Unit 3 Single Line Test Report and Data Evaluation," January 2011. (Proprietary)

4-6 Fauske and Associates Report, FAI/10-507, Rev. 0, "South Texas (STP) Unit 3 Supplemental Test Report for 4 Loop Acoustic Model," November 2010. (Proprietary)

5 DRYER STARTUP INSTRUMENTATION AND STRUCTURAL EVALUATION

In order to determine the acoustic loads acting on the STP steam dryer and the associated dryer stresses, the dryer will be instrumented with a collection of pressure transducers (PTs), strain gages (SGs) and accelerometers. This section documents the methodology and instrumentation to be used for the STP Unit 3 steam dryer stress monitoring during the power ascension to 100%. [

]a,c

Steam dryer stress estimation is a [ ]a,c. The [

]a,c

For this reason, the [

]a,c

In addition to describing the general methodology, this discussion delineates the locations of the various sensors used and provides reasons for their selection. The instrumentation for the STP Unit 3 dryer consists of [ ]a,c PTs and [ ]a,c SGs with [ ]a,c accelerometers intended to monitor [ ]a,c The selection of the PT locations is based on a combination of [

]a,c

The following sections describe the overall methodology and details concerning key aspects of its numerical implementation. This is followed by a summary and accompanying discussion regarding the placement of the [ ]a,c for collecting the data needed to estimate the MSL entrance pressures. Results are also presented recording the rank and condition number (an indication of how well the MSL entrance signals can be measured for a given sensor suite) of the least squares estimation method as a function of frequency.

5.1 FINITE ELEMENT MODEL

The STP steam dryer FEM was built with ANSYS® Version 11 and is shown in Figure 5.1-1. The FEM consists of mostly [ ]a,c
The model has [ ]a,c nodes and [ ]a,c elements. Details of the development of the FEM are documented in Reference 5-1.

[a,c

[

]a,c The model is separated into many elements. Generally, these components have boundaries at welds.

The dryer structure consists of [

]a,c are shown in Figure 5.1-8.

The [

]a,c The lifting lug arrangement is shown in Figure 5.1-11.

Finite Element Model Mesh and Connectivity

The dryer plates are all modeled [

]a,c

The vane bank [

]a,c

[ ]a,c

Vane Bank Representation

The vane bank modules are box-like structures with many internal hanging chevrons. [

]a,c The perforated

plates [

]a,c

Figure 5.1-14 shows the [

]a,c

Lifting Rod Representation

The lifting rod itself is modeled [

]a,c are shown in Figure 5.1-12. [

]a,c

Dryer Skirt Submerged in Water

The dryer skirt is partially submerged in water. The skirt and drain channel components are separated into groups above and below the water line. The acoustic loading is only applied to elements above the water line. The material density for the stainless steel below water has been adjusted to account for the effect of the hydrodynamic mass.

a,c

Figure 5.1-1 Steam Dryer FEM

[ ]a,c

Figure 5.1-2 [ ]a,c

a,c

Figure 5.1-3 [ ]a,c

a,c

Figure 5.1-4 Vane Bank [ ]a,c

[ ]a,c

Figure 5.1-5 Vane Bank Mass Blocks

[ ]a,c

Figure 5.1-6 [ ]a,c

a,c

Figure 5.1-7 Hood Supports

a,c

Figure 5.1-8 Hoods

a,c

Figure 5.1-9 Dryer Viewed From Below

a,c

Figure 5.1-10 Skirt and Drain Ducts

a,c

Figure 5.1-11 Lifting Rods

a,c

Figure 5.1-12 Moment Transfer Beams

a,c

Figure 5.1-13 Vane Bank Details

a,c

Figure 5.1-14 Solid Element Vane Bank Mass Blocks

5.1.1 Modal Analysis

As part of the preoperational and startup testing for the RJ-ABWR, a hammer test was performed to identify the as-built frequencies and mode shapes of several key components of the dryer at ambient environment conditions. Because the STP Unit 3 steam dryer is essentially identical to the RJ-ABWR, the results of the RJ-ABWR hammer test can be compared to the modal analysis results for the STP Unit 3 steam dryer.

A modal analysis has been performed for the STP Unit 3 dryer that incorporates the same boundary conditions as the hammer test of the RJ-ABWR for the purpose of comparing analytical and test results. The dryer components that were compared include the outer and middle hoods, cover plate (270-degree side with no manhole cover), skirt, and drain channel. Details of the modal analysis and comparison to the RJ-ABWR hammer test results are documented in Reference 5-2. Table 5.1-1 provides a summary of the comparison between the hammer test results and the STP Unit 3 analytical results. This comparison between the RJ-ABWR hammer test results and the STP FEM modal analysis results show that the STP FEM provides a realistic representation of the actual dryer.

Table 5.1-1 Comparison of RJ-ABWR Hammer Test and STP Modal Analysis Results

a,c

5.2 DRYER INSTRUMENTATION METHODOLOGY

The STP steam dryer will be instrumented with [ ]a,c PTs, [ ]a,c accelerometers and [ ]a,c SGs. In addition, SG measurements at [ ]a,c locations on each of the MSLs will also be recorded to indirectly measure the dynamic pressure responses at those locations, though the intent of that data is for information purposes only. Using the methodology described in the following sections, it is planned to use the collected data to estimate the stresses on the steam dryer and quantify the biases and uncertainties attached to this estimate. The data are also available to address a secondary objective of [

]a,c

5.2.1 Methodology

[ ]a,c

5.2.2 [ ]a,c

[ ]a,c

a,c

Figure 5.2.2-1 Steam Dryer Schematic with One MSL Entrance

a,c

Figure 5.2.2-2 [**]a,c**

a,c

a,c

a,c

a,c

5.2.3 Application to Strain Gage Measurements

a,c

a,c

5.2.4 Numerical Implementation Details

a,c

a,c

[ ]a,c

Figure 5.2.4-1(a) [ ]a,c

Note: [ ]a,c

a,c

Figure 5.2.4-1(b) [

]a,c

[ ]a,c

Figure 5.2.4-2(a) [ ]a,c

a,c

Figure 5.2.4-2(b) [

]a,c

[ ]a,c

Figure 5.2.4-3(a) [ ]a,c

a,c

Figure 5.2.4-3(b) [

]a,c

[a,c

Figure 5.2.4-4(a) [

]a,c

a,c

Figure 5.2.4-4(b) [

]a,c

a,c

Figure 5.2.4-5(a) [

]a,c

a,c

Figure 5.2.4-5(b) [

]a,c

5.2.5 Stress Evaluation for Instrumentation

a,c

a,c

5.2.6 Application of Frequency Shifting and Biases and Uncertainties

a,c

a,c

5.3 DRYER INSTRUMENTATION

This section describes the sensor types and locations for the STP Unit 3 dryer.

5.3.1 Pressure Transducers

a,c

[ ] a,c

Redundancy

[ ] a,c

Table 5.3.1-1 PT Locations

a,c

a,c

Figure 5.3.1-1 RJ-ABWR Steam Dryer Instrumentation

a,c

Figure 5.3.1-2 PT Locations [ ][a,c]

a,c

a,c

Figure 5.3.1-3 PT Locations [ ]a,c

a,c

5.3.2 SG Locations

a,c

a,c

Table 5.3.2-1 Strain Gage Locations

a,c

a,c

Figure 5.3.2-1 [ ][a,c]

a,c

Figure 5.3.2-2 [

] a,c

a,c

Figure 5.3.2-3 Strain Gage Locations [ ]a,c

The stress contours represent estimated alternating stresses.

a,c

Figure 5.3.2-4 Strain Gage Locations [ ]a,c

The stress contours represent estimated alternating stresses.

5.3.3 Accelerometer

a,c

Table 5.3.3-1 Accelerometer Locations

a,c

Figure 5.3.3-1 Accelerometer Locations

5.4 RESULTS OF INSTRUMENTATION EVALUATION

a,c

5.4.1 Condition Number and Rank for PT Arrangement

a,c

a,c

Table 5.4.1-1 Condition Numbers and Frequency for PT Sensor Arrangement 1

a,c

a,c

Figure 5.4.1-1 Condition Number Variation with Frequency for PT Sensor Arrangement 1

a,c

a,c

Figure 5.4.1-2 Rank Calculated in SGELSS using RCOND=0.01

5.4.2 Condition Number and Rank for SG Arrangement

a,c

Table 5.4.2-1 Condition Numbers and Frequency for SG Sensor Arrangement

a,c

a,c

Figure 5.4.2-1 Condition Number Variation with Frequency for SG Sensor Arrangement

5.5 STRUCTURAL EVALUATION USING RJ-ABWR STARTUP DATA

A structural evaluation of the STP steam dryer was performed (Reference 5-14) using the RJ-ABWR startup data to determine the fluctuating pressure loads induced by the flowing steam. The main basis for qualification of the STP steam dryer remains the operating experience, which is described in Section 3. However, a stress analysis consistent with those carried out in the U.S. for prior dryer qualification to EPU conditions has been performed for the STP steam dryer, and the resulting stresses are assessed for compliance with the ASME B&PV Code 2007 (Reference 5-10), Section III, subsection NG, for the load combination corresponding to normal operation (the Level A Service Condition).

5.5.1 Structural Evaluation Overview

[

]a,c In this regard the evaluation differs from the procedure used in existing plants where an acoustic circuit analysis of the steam dome and MSLs is used in combination with pressure measurements on the MSL to infer the acoustic loads. Moreover, these dryer measurements are only available in the form of RMS measurements so that phase information on the individual sensors is unavailable. [

]a,c

[

]a,c

The MSL acoustic load stress evaluation consists of applying the acoustic load estimates to a FEM of the STP steam dryer. The unit solution stresses were developed by imposing the unit solution acoustic pressures obtained using Helmholtz solution algorithms on the finite element dryer model. The finite element nodal stresses are developed by combining the unit solution stresses with the MSL signals, and comparing the stresses against the appropriate endurance limits to establish the structural adequacy of the dryer.

This report describes the overall methodology used to obtain the unit solutions in the frequency domain and how to assemble them into a stress response for a given combination of pressure signals in the MSLs. This is followed by a description of the application of these acoustic loads to the STP steam dryer FEM. Deadweight stresses are described herein together with the post-processing procedures, computation of maximum and alternating stress intensities, identification of high stress locations, adjustments to stress intensities at welds and evaluation of stress ratios used to establish compliance with the ASME Code. The results for stress intensity distributions and stress ratios are presented with PSDs of the dominant stress components in Section 5.5.5.

5.5.2 Methodology

Based on EPU operating conditions, the steam dryer can experience strong acoustic loads due to the fluctuating pressures in the MSLs connected to the steam dome containing the dryer. A frequency-based acoustic loads prediction methodology has been developed that, given the MSL inlet pressures, determines the acoustic field everywhere inside the steam dome. In prior steam dryer evaluations, the MSL signals have been determined using a collection of strain gage measurements of the fluctuating pressures in the MSLs and an ACM. [

]a,c After the MSL signals are determined, the stress evaluation proceeds by combining the unit solutions with the MSL signals described in Section 5.5.2.2.

5.5.2.1 Development of Dryer Loads from RJ-ABWR Spectra Data

[

]a,c

This section summarizes the solution approach and presents comparisons between predictions and measurements on the RJ-ABWR dryer.

Data were collected on the RJ-ABWR dryer at 100% power for the following:

[ ]a,c

The specific locations of interest are summarized in Table 5.5.2.1-1 and shown in Figure 5.5.2.1-1.

Table 5.5.2.1-1 Applicable RJ-ABWR Steam DryerMeasurement Descriptions and Locations

a,c

[ ]a,c

Figure 5.5.2.1-1 [ ]a,c

[ ]a,c

a,c

[ ]a,c

Converting the [ ]a,c from the ANSYS® results into [ ]a,c gives the comparisons with data shown in Figures 5.5.2.1-2 to 5.5.2.1-15. Note that when the prediction matches the measurement, the black curve is obscured by the red curve. PSDs of the entrance pressures are shown in Figure 5.5.2.1-16.

a,c

Figure 5.5.2.1-2 Comparison of Acceleration Data Collected on RJ-ABWR with Model Predictions for the A1 Accelerometer

The vertical scale is in units of 0.001 times gravity.

a,c

Figure 5.5.2.1-3 Comparison of Displacement Data Collected on RJ-ABWR with Model Predictions for the A2 Accelerometer

The vertical scale is in units of 0.001 inches.

a,c

Figure 5.5.2.1-4 Comparison of Displacement Data Collected on RJ-ABWR with Model Predictions for the A3 Accelerometer

The vertical scale is in units of 0.001 inches.

a,c

Figure 5.5.2.1-5 Comparison of Displacement Data Collected on RJ-ABWR with Model Predictions for the A4 Accelerometer

The vertical scale is in units of 0.001 inches.

a,c

Figure 5.5.2.1-6 Comparison of Strain Data Collected on RJ-ABWR with Model Predictions for the S1 Strain Gage

The vertical scale is in units of 10^{-9} inches per inch.

a,c

Figure 5.5.2.1-7 Comparison of Strain Data Collected on RJ-ABWR with Model Predictions for the S2 Strain Gage

The vertical scale is in units of 10^{-9} inches per inch.

a,c

Figure 5.5.2.1-8 Comparison of Strain Data Collected on RJ-ABWR with Model Predictions for the S3 Strain Gage

The vertical scale is in units of 10^{-6} inches per inch.

a,c

Figure 5.5.2.1-9 Comparison of Strain Data Collected on RJ-ABWR with Model Predictions for the S4 Strain Gage

The vertical scale is in units of 10^{-6} inches per inch.

a,c

Figure 5.5.2.1-10 Comparison of Strain Data Collected on RJ-ABWR with Model Predictions for the S5 Strain Gage

The vertical scale is in units of 10^{-6} inches per inch.

a,c

Figure 5.5.2.1-11 Comparison of Strain Data Collected on RJ-ABWR with Model Predictions for the S6 Strain Gage

The vertical scale is in units of 10^{-6} inches per inch.

a,c

Figure 5.5.2.1-12 Comparison of Strain Data Collected on RJ-ABWR with Model Predictions for the S7 Strain Gage

The vertical scale is in units of 10^{-6} inches per inch.

a,c

Figure 5.5.2.1-13 Comparison of Strain Data Collected on RJ-ABWR with Model Predictions for the P3 Pressure Transducer

The vertical scale is in units of 0.001 psid.

a,c

Figure 5.5.2.1-14 Comparison of Strain Data Collected on RJ-ABWR with Model Predictions for the P4 Pressure Transducer

The vertical scale is in units of 0.001 psid.

a,c

Figure 5.5.2.1-15 Comparison of Strain Data Collected on RJ-ABWR with Model Predictions for the P5 Pressure Transducer

The vertical scale is in units of 0.001 psid.

a,c

Figure 5.5.2.1-16 Predicted MSL Entrance Source Pressures - PSD

Figure 5.5.2.1-10 shows (for example) that the [

]a,c

5.5.2.1.1 Bias and Uncertainty

The bias and uncertainty values that are applied to the RJ-ABWR dryer from the acoustic analysis consist of the [

]a,c These values are combined with applicable values determined from previous analyses on BWR dryers, and are shown in Table 5.5.2.1-2.

Table 5.5.2.1-2 [**]a,c**

a,c

Bias and uncertainty values are taken from Reference 5-14. [

]a,c

5.5.2.2 Evaluation of Unit Solutions

a,c

[ ]a,c

5.5.2.3 [ ]a,c

[ ]a,c

a,c

5.5.2.4 Computational Considerations

a,c

Structural Damping

a,c

a,c

Evaluation of Alternating Stress Intensities

a,c

5.5.2.5 Pressure Loading

The harmonic loads are produced by the pressures acting on the exposed surfaces of the steam dryer. [

]a,c

As described in Section 5.5.2, [

]a,c This is useful since revisions in the loads model do not necessitate recalculation of the unit stresses.

a,c

Figure 5.5.2.5-1(a) [

]a,c

[ ]a,c

a,c

Figure 5.5.2.5-1(b) [

]a,c

[ ]a,c

a,c

Figure 5.5.2.5-1(c) [

]a,c

[ ]a,c

5.5.3 MSL Acoustic Structural Analysis

a,c

5.5.3.1 Static Analysis

The results of the static analysis are shown in Figure 5.5.3.1-1. [ ]a,c This value overestimates the actual level due to unrealistically high stress concentrations in the finite element model at structural discontinuities.

5.5.3.2 Harmonic Analysis

The harmonic pressure loads were applied to the structural model at all surface nodes [ ]a,c Stresses were calculated for each frequency and results from static and harmonic calculations were combined as described in Section 5.5.2.4, Equation (22).

5.5.3.3 Post-Processing

a,c

a,c

Figure 5.5.3.1-1 [

]a,c

a,c

The maximum stresses are compared against allowable values which depend upon the stress type (membrane, membrane+bending, alternating – Pm, Pm+Pb, S_{alt}) and location (at a weld or away from welds). These allowable values are specified in the following section. For solid elements the most conservative allowable value for membrane stress, Pm, is used, although bending stresses are also nearly always present. The structure is then assessed in terms of stress ratios formed by dividing allowable values by the computed stresses at every node. Stress ratios less than one indicates that the associated maximum and/or alternating stress intensities exceed the allowable levels.

5.5.3.4 Structural Assessment - Acoustic

The ASME B&PV Code (Reference 5-10), Section III, subsection NG provides different allowable stresses for different load combinations and plant conditions. The stress levels of interest in this analysis are for the normal operating condition, which is the Level A service condition. The load combination for this condition is:

Normal Operating Load Combination = Weight + Pressure + Thermal

The weight and fluctuating pressure contributions have been calculated in this analysis and are included in the stress results. [

]^{a,c}

5.5.3.5 Allowable Stress Intensities

The ASME B&PV Code (Reference 5-10), Section III, subsection NG specifies the maximum allowable stress intensity (Sm) and alternating stress intensity (Sa) for the Level A service condition. The calculation for different stress categories is performed in accordance with Figure NG-3221-1 of Division I, Section III, subsection NG.

The maximum allowable stress intensities are listed below in Table 5.5.3.4-1 and are taken from Table I-1.2 of the ASME B&PV Code (Reference 5-10) for 316L steel plate. The allowable value for alternating stress intensities for austenitic steels at an operating temperature of 576°F, according to Table I-9.2.2, and Figure I-9.2.2 (Curve C) in Appendix I of Section III of the ASME B&PV Code, is 13.6 ksi. This value corresponds to a Young's modulus of $E=28.3\times10^6$ psi. According to NG-3222.4 in subsection NG of Section III of the ASME Code (Reference 5-10), the effect of elastic modulus upon alternating stresses is taken into account by multiplying alternating stress S_{alt} at all locations by the ratio, $E/E_{model}=1.1$, where:

$E = 28.3\times10^6$ psi, as shown on Fig. I-9.2.2 of the ASME BP&V Code

$E_{model} = 25.425\times10^6$ psi (Reference 5-15)

[

]^{a,c}

Table 5.5.3.4-1 Maximum Allowable Stress Intensities and Alternating Stress Endurance Limit

Type	Notation	Service Limit	Allowable Value (ksi)
Maximum Stress Allowables:			
General Membrane	Pm	Sm	13.7
Membrane + Bending	Pm + Pb	1.5 Sm	20.6
Primary + Secondary	Pm + Pb + Q	3.0 Sm	41.1
Alternating Stress Allowable:			
Peak = Primary + Secondary + F	S_{alt}	Sa	9.95

The notation Pm represents membrane stress; Pb represents stress due to bending; Q represents secondary stresses (from thermal effects and gross structural discontinuities, for example); and F represents additional stress increments (due to local structural discontinuities, for example).

5.5.3.6 Adjustments to Stresses and Stress Allowables on Welds

At a weld, the stress evaluation is modified to account for stress concentration occurring in the weld, variability in the weld quality and the degree of inspection performed upon the post-fabrication dryer. The adjustment is performed in accordance with Table NG-3352-1 in the ASME B&PV Code (Reference 5-10). [

]^{a,c}

5.5.3.7 Computation of Stress Ratios

The following quantities are computed at every node:

1. The maximum membrane stress intensity, Pm (evaluated at the mid-thickness location for shells).

2. The maximum membrane+bending stress intensity, Pm+Pb, (taken as the largest of the maximum stress intensity values at the bottom, top, and mid thickness locations, for shells).

3. The alternating stress, S_{alt}, [ ]^{a,c}

4. The stress ratio due to a maximum stress intensity assuming the node lies at a non-weld location (note that this is the maximum ratio obtained considering both membrane stresses and membrane+bending stresses):

   SR-P(nw) = min{ Sm/Pm, 1.5 * Sm/(Pm+Pb) }.

5. The alternating stress ratio assuming the node lies at a non-weld location,

   SR-a(nw) = Sa / S_{alt}

6. The same as 4, but assuming the node lies on a weld,

   SR-P(w) = SR-P(nw) * n (n=0.5 for full penetration weld)

7. The same as 5, but assuming the node lies on a weld,

   SR-a(w) = SR-a(nw) / f (f=2 for full penetration weld)

Note that in steps 4 and 6, the minimum of the stress ratios based on P_m and P_m+P_b is taken. The allowable values listed in 5.5.3.4-1 are Sm=13.7 ksi and [ ]^{a,c} The factors, n and f are the weld quality and fatigue factors discussed above with the default values, n=0.5 and f=2, being appropriate for a full penetration weld.

The appropriate maximum and alternating stress ratios for the acoustic loads, SR-P and SR-a, are thus determined and a final listing of nodes having the smallest stress ratios is generated. [The non-MSL acoustic stresses are conservatively combined to the acoustic stress results for only the location with the smallest stress ratio. The nodes with stress ratios lower than 4 are plotted,and these nodes are tabulated and depicted in Section 5.5.5.]^{a,c}

5.5.4 Non-MSL Acoustic Loads

[ ]^{a,c}

5.5.4.1 Review of RJ-ABWR MSL Data

[ ]a,c

5.5.4.2 Resonance of the Annular Cavity of the Skirt

[ ]a,c

5.5.4.3 Structural Evaluation – Non-MSL Acoustic

[ ]a,c

Approach

Modal analyses were performed to calculate frequencies, mode shapes, stresses, mode participation factors for uniform loads, modal stresses and displacements at the locations of sensors used in the RJ-ABWR startup tests, and maximum modal stresses in the dryer skirt and drain channels for the 0-100 Hz frequency range corresponding to measurement frequency content of the measured strains and displacements. The calculated modal strains/displacements at the sensor locations were related to the maximum modal stresses in the components. [

]a,c

[ ]a,c

a,c

[a,c]

Loads

Analyses are based on strain and displacement measurements at strain gages and accelerometers mounted on the skirt and drain channels during RJ-ABWR startup testing. Relevant sensors and their locations on the dryer are shown in Figure 5.3.1-1. [

]a,c

Table 5.5.4.3-1 p-p Values from Sensor Time Histories

[a,c]

Analysis Model

The analysis was performed using the FEM derived from a full dryer analysis model described in Section 5.1. The model used in the analysis (Figure 5.5.4.3-1) consisted of the dryer skirt, drain channels, upper

support ring, and bottom stiffening ring. Analyses were limited to these components based on the following considerations.

The dryer model is a comprehensive model of the whole dryer resulting in a very large number of closely spaced vibration modes. [ ]a,c

a,c

Stress Calculations

a,c

Table 5.5.4.3-2 [ ][a,c]

[ ]a,c

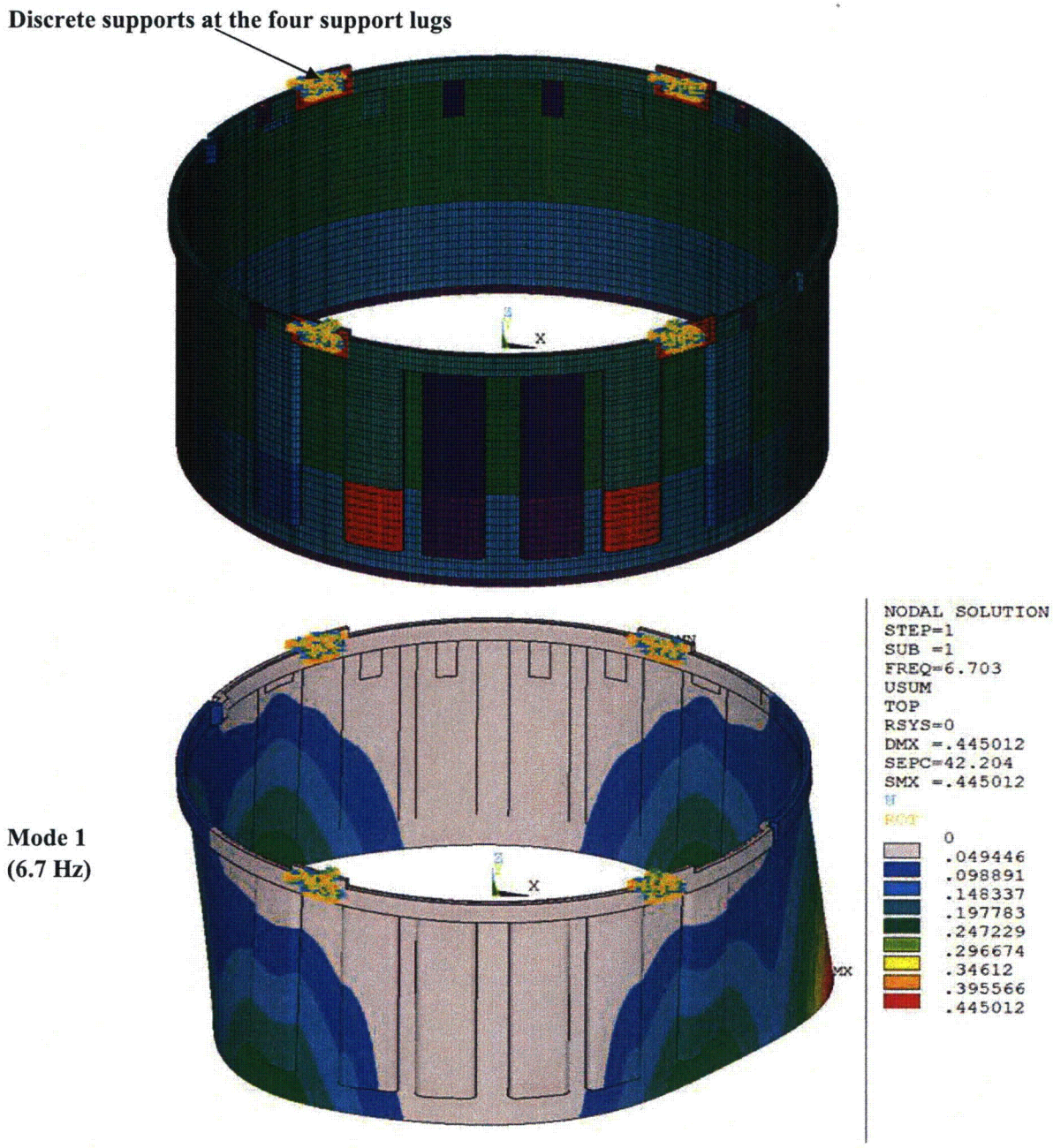

Figure 5.5.4.3-1 Skirt, Drain Channel, and Support Ring Model With Discrete Supports at Four Support Lugs

5.5.5 Results

The estimated stress intensities and associated stress ratios resulting from the application of the acoustic/hydrodynamic loads are presented below. In the following sections the highest maximum and alternating stress intensities are presented to indicate which points on the dryer experience significant stress concentration and/or modal response (Section 5.5.5.1). The lowest stress ratios obtained by comparing the calculated stresses against allowable values, accounting for stress type (maximum and alternating) and location (on or away from a weld), are also reported (Section 5.5.5.2). [

]a,c

5.5.5.1 General Stress Distribution and High Stress Locations

The maximum stress intensities obtained by post-processing the stresses on the STP steam dryer at 100% power are listed in Table 5.5.5.1-1. Contour plots of the stress intensities over the steam dryer structure are shown in Figures 5.5.5.1-1 through 5.5.5.1-5. The figures are oriented to emphasize the high stress regions. Note that these stress intensities do not account for weld factors. Further, it should be noted that

since the allowable stresses vary with location, stress intensities do not necessarily correspond to regions of primary structural concern. Instead, structural evaluation is more accurately made in terms of the stress ratios which compare the computed stresses to allowable levels with due account made for stress type and weld.

a,c

Table 5.5.5.1-1 Locations with Highest Predicted Stress at 100% Power

a,c

[ ]a,c

Figure 5.5.5.1-1 [ ]a,c

[ ]a,c

[ ]a,c

Figure 5.5.5.1-2 [

]a,c

[ ]a,c

[a,c]

Figure 5.5.5.1-3 [

]a,c

[

]a,c

[ ]a,c

Figure 5.5.5.1-4 [ ]a,c

[ ]a,c

a,c

Figure 5.5.5.1-5 [ ][a,c]

5.5.5.2 Load Combinations and Allowable Stress Intensities

The stress ratios computed for 100% power operation are contained in Tables 5.5.5.2-1 through 5.5.5.2-3. The stress ratios are grouped according to type (SR-P for maximum membrane and membrane+bending stress, SR-a for alternating stress) and location (away from welds or at a weld). The tabulated nodes are also depicted in Figures 5.5.5.2-1 through 5.5.5.2-10. The plots for non-weld locations depict all nodes with stress ratios of [ ]^{a,c} The nodes listed in Tables 5.5.5.2-1 and 5.5.5.2-3 appear as larger spheres in Figures 5.5.5.2-1 through 5.5.5.2-10 and are numbered according to the entry in the table.

[

]^{a,c}

Table 5.5.5.2-1 Limiting Non-weld Locations with at 100% Power Operating Condition

a,c

Stress ratios are grouped according to stress type (maximum – SR-P; or alternating – SR-a). Locations are depicted in Figures 5.5.5.2-1 through 5.5.5.2-4.

Table 5.5.5.2-2 Limiting Peak Stress Ratios, SR-P, on Welds at 100% Power Operating Condition

a,c

Locations are depicted in Figures 5.5.5.2-5 through 5.5.5.2-8.

Table 5.5.5.2-3 Limiting Alternating Stress Ratios, SR-a, on Welds at 100% Power Operating Condition

a,c

Gray cells indicates minimum stress ratio on the structure. Locations are depicted in Figures 5.5.5.2-9 and 5.5.5.2-10.

a,c

Figure 5.5.5.2-1 Locations of Limiting Peak Stress Ratios, [ ]a,c, at Non-Welds – Location 1

Large spheres correspond to locations in Table 5.5.5.2-1.

a,c

Figure 5.5.5.2-2 Locations of Limiting Peak Stress Ratios, [ ]^{a,c}, at Non-Welds – Locations 2 and 3

Large spheres correspond to locations in Table 5.5.5.2-1.

a,c

Figure 5.5.5.2-3 Locations of Limiting Alternating Stress Ratios, [ ]^{a,c}, at Non-Welds – Locations 1-5

Large spheres correspond to locations in Table 5.5.5.2-1.

a,c

Figure 5.5.5.2-4 Locations of Limiting Alternating Stress Ratios, [ ]^{a,c}, at Non-Welds

Large spheres correspond to locations in Table 5.5.5.2-1. Figure 5.5.5.2-4 shows stresses on side opposite that shown in Figure 5.5.5.2-3.

a,c

Figure 5.5.5.2-5 Locations of Limiting Stress Ratios, [ ]a,c, at Welds

Large spheres correspond to locations in Table 5.5.5.2-2. Locations 1, 3, 4 and 7 through 9.

a,c

Figure 5.5.5.2-6 Locations of Limiting Stress Ratios, [ ]a,c, at Welds

Large spheres correspond to locations in Table 5.5.5.2-2. Figure 5.5.5.2-7 shows locations 2, 3, 11, 12, and 14.

a,c

Figure 5.5.5.2-7 Locations of Limiting Stress Ratios, [ ]^{a,c}, at Welds

Large spheres correspond to locations in Table 5.5.5.2-2. Figure 5.5.5.2-7 shows locations 1, 4, 5, 8, 9 and 13.

a,c

Figure 5.5.5.2-8 Locations of Limiting Alternating Stress Ratios, [ ]a,c, at Welds

Large spheres correspond to locations in Table 5.5.5.2-2. Figure 5.5.5.2-8 shows locations 2, 5, 6, 10 and 13.

a,c

Figure 5.5.5.2-9 Locations of Limiting Alternating Stress Ratios, [ ]a,c, at Welds

Large spheres correspond to locations in Table 5.5.5.2-3. Figure 5.5.5.2-9 shows locations 1through 4, 6 through 9 and 11.

a,c

Figure 5.5.5.2-10 Locations of Limiting Alternating Stress Ratios, [ ]a,c, at Welds

Large spheres correspond to locations in Table 5.5.5.2-3. Figure 5.5.5.2-10 shows locations 5 and 10.

5.5.5.3 Frequency Content and Filtering of the Stress Signals

a,c

These are the nodes labeled 1, 3, 5, 7, 10 and 11 in Table 5.5.5.2-3 for alternating stresses on a weld and accompanying Figures 5.5.5.2-1 through 5.5.5.2-10.

a,c

a,c

a,c

Figure 5.5.5.3-1 Accumulative PSD and PSD Curves of the σ_{yy} Stress Response at Node 128691; Dominant Frequency: 59.5 Hz

a,c

Figure 5.5.5.3-2 Accumulative PSD and PSD of the σ_{zx} Stress Response at Node 103032; Dominant Frequency: 95.1 Hz

a,c

Figure 5.5.5.3-3 Accumulative PSD and PSD of the σ_{xx} Stress Response at Node 83569; Dominant Frequency: 15.1 Hz

a,c

Figure 5.5.5.3-4 Accumulative PSD and PSD of the σ_{zz} Stress Response at Node 3053; Dominant Frequency: 20.1 Hz

a,c

Figure 5.5.5.3-5 Accumulative PSD and PSD of the σ_{zz} Stress Response at Node 84160; Dominant Frequency: 15.1 Hz

a,c

Figure 5.5.5.3-6 Accumulative PSD and PSD of the σ_{zz} Stress Response at Node 102649; Dominant Frequency: 18.0 Hz

a,c

Figure 5.5.5.3-7 Contour Map Showing the Dominant Frequencies (0-25 Hz)

Figure 5.5.5.3-7 shows locations with dominant frequencies (i.e., the frequency with the largest stress harmonic) in the range of 0-25 Hz.

a,c

Figure 5.5.5.3-8 Contour Map Showing the Dominant Frequencies (25-75 Hz)

Figure 5.5.5.3-8 shows locations with dominant frequencies (i.e., the frequency with the largest stress harmonic) in the range of 25-75 Hz.

a,c

Figure 5.5.5.3-9 Contour Map Showing the Dominant Frequencies (75-200 Hz)

Figure 5.5.5.3-9 shows locations with dominant frequencies (i.e., the frequency with the largest stress harmonic) in the range of 75-200 Hz.

5.6 SUMMARY

The methodology for placing pressure transducers, strain gages, and accelerometers on the STP Unit 3 dryer and evaluating their effectiveness in estimating the MSL entrance sources have been described in the preceding sections.

The PT sensor arrangement has [

]a,c

An arrangement of SG sensors is also presented and evaluated. [

]a,c

A frequency-based steam dryer stress analysis has been used to obtain best estimates of the high stress locations and stress ratios for the STP steam dryer at 100% power conditions using [

]a,c

[

]a,c

5.7 REFERENCES FOR SECTION 5

5-1 Westinghouse Calculation, CN-A&SA-10-37, Rev. 0, "South Texas Project Steam Dryer Finite Element Model," October 2010. (Proprietary)

5-2 Westinghouse Calculation, CN-A&SA-10-48, Rev. 1, "STP Steam Dryer Modal Analysis Comparison to K6 Hammer Test Results," December 2010. (Proprietary)

5-3 Continuum Dynamics, Inc. Report No. 07-09P, Revision 1, "Methodology to Predict Full Scale Steam Dryer Loads from In-Plant Measurements, with the Inclusion of a Low Frequency Hydrodynamic Contribution," July 2007. (Proprietary)

5-4 Fauske and Associates Report, FAI/10-507, Rev. 0, "South Texas (STP) Unit 3 Supplemental Test Report for 4 Loop Acoustic Model," November 2010. (Proprietary)

5-5 Fauske and Associates Report, FAI/10-547, Rev. 0, "South Texas (STP) Unit 3 Supplemental Test Report for 4 Loop Acoustic Model – Data Evaluation," November 2010. (Proprietary)

5-6 Toshiba Corporation Document No. RS-5126954, Rev. 1, "Prototype ABWR Reactor Internals Flow Induced Vibration Test Report," 2008. (Proprietary)

5-7 LAPACK Driver Routine (Version 3). University of Tennessee, University of California at Berkley, NAG Ltd., Courant Institute, Argonne National Laboratory, and Rice University, 1999.

5-8 ANSYS®, Release 10.0 Complete User's Manual Set, (http://www.ansys.com).

5-9 Westinghouse Calculation, CN-A&SA-10-46, Rev. 1, "Generation of Three-Dimensional Acoustic Solutions for South Texas Project Units 3 & 4 Compatible with Continuum Dynamics Inc. Analysis Methods," November 2010. (Proprietary)

5-10 ASME Boiler and Pressure Vessel Code, Section III, Subsection NG (2007).

5-11 Continuum Dynamics, Inc. White Paper No. 10-24P, Rev. 3, "Approach for Assessing Full Scale STP Steam Dryer Structural Margin at 100% Power, Including Power Ascension," 2010. (Proprietary)

5-12 Continuum Dynamics, Inc. Technical Note No. 11-02P, Rev. 0, "Data Comparison for the STP Dryer at 100% Power, Based on Pressure Transducer Measurements on a Subscale Model," 2011. (Proprietary)

5-13 Westinghouse Letter, LT-RIDA-10-294, Rev. 0, "Recommended Damping Ratio, Peak-to-RMS Ratio, and Stress Concentration Factor Application for ABWR Reactor Internals Flow-Induced Vibration Analysis," 10/28/2010. (Proprietary)

5-14 Continuum Dynamics, Inc. Report No. 11-06P, Rev. 0, "Stress Assessment of South Texas Project Steam Dryer at 100% Power Using Full Scale RMS Measurement," 2011. (Proprietary)

5-15 Westinghouse Calculation, CN-A&SA-10-37, Rev. 0, "South Texas Project Steam Dryer Finite Element Model," October 2010. (Proprietary)

5-16 XGEN Report, XGEN-2011-03, Rev. 0, "Conversion of Kashiwazaki-Kariwa Unit 6 'Peak Hold'

Spectra," February 2011. (Proprietary)

5-17 Toshiba Corporation Document No. PDR-2011-100371, Rev. 0, "Vibration Measurement Report of K-6 Main Steam Lines," 2011. (Proprietary)

5-18 Toshiba Corporation Document No. RS-5152567, Rev. 1, "Simple Overview for the resonance in the annular cavity of the outer skirt," 2011. (Proprietary)

5-19 XGEN Report, XGEN-2011-10, Rev. 0, "Stress Analysis of STP Dryer Skirt Assembly for Low Frequencies," June 2011.

This page left intentionally blank.

6 STEAM DRYER POWER ASCENSION PLAN

6.1 APPROACH - OVERVIEW

The following sections (details provided in Reference 6-1) describe the power ascension plan for the steam dryer will include an initial hold point at [ ]a,c power to collect steam dryer data and generate limit curves to ensure that the steam dryer stresses are below the fatigue limit. At [ ]a,c power, the flow is approximately [ ]a,c at 100% thus; no acoustic resonance is expected to occur. Thereafter, for every 10% power increment up to 100% power, the plant will hold power to collect steam dryer data and generate limit curves.

[ ]a,c

The following sections describe

- Limit curve methodology
- Power ascension process
- Validation of the use of steam dryer pressure data
- Biases and uncertainties

6.2 LIMIT CURVE METHODOLOGY

a,c

Figure 6.2-1 Schematic of the Solution Field

a,c

a,c

6.3 POWER ASCENSION PROCESS

To ensure that the dryer stresses are within acceptable limits, the following process will be used during initial startup power ascension:

a,c

a,c

6.4 VALIDATION OF THE USE OF [ ]a,c

[ ]a,c

These results give qualitative confidence that the methodology will provide an accurate representation of the [ ]a,c loads on the dryer.

a,c

Figure 6.4-1 Schematic of the Subscale PT Locations IDP1 to IDP12 (Reference 6-5)

a,c

Figure 6.4-2 Schematic of the [ ]a,c

a,c

a,c

Figure 6.4-3 [

]a,c

a,c

Figure 6.4-4 [

]a,c

a,c

Figure 6.4-5 [

]a,c

a,c

Figure 6.4-6 [

]a,c

6.5 BIASES AND UNCERTAINTIES

a,c

6.5.1 Bias and Uncertainty at [ ]a,c Power

a,c

a,c

Table 6.5-1 Bias and Uncertainty for [ ]a,c

a,c

[a,c

Figure 6.5-1 [

]a,c

a,c

Figure 6.5-2 [

]a,c

[a,c

Figure 6.5-3 [

]a,c

a,c

Figure 6.5-4 [

]a,c

6.6 REFERENCES FOR SECTION 6

6-1 Continuum Dynamics, Inc. Technical Note No. 11-03P, "Methodology and Plan for Monitoring STP Steam Dryer Performance During Power Ascension," February 2011. (Proprietary)

6-2 LAPACK Driver Routine (Version 3.0). 10/31/1999. University of Tennessee, University of California at Berkeley, NAG Ltd., Courant Institute, Argonne National Laboratory, and Rice University.

6-3 Anderson, E., Z. Bai, C. Bischof, J. Demmel, J. Dongarra, J. Du Croz, A. Greenbaum, S. Hammarling, A. McKenney, S. Ostrauchov, and D. Sorensen. 1992. LAPACK Users Guide. Society for Industrial and Applied Mathematics (SIAM): Philadelphia, PA.

6-4 Westinghouse Calculation, CN-A&SA-10-31, Rev. 1, "South Texas Unit 3 Scaling to Four Line Subscale Model," July 2010. (Proprietary)

6-5 Fauske and Associates Report, FAI/10-507, Rev. 0, "South Texas (STP) Unit 3 Supplemental Test Report for 4 Loop Acoustic Model," November 2010. (Proprietary)

6-6 Fauske and Associates Report, FAI/10-547, Rev. 0, "South Texas (STP) Unit 3 Supplemental Test Report for 4 Loop Acoustic Model – Data Evaluation," November 2010. (Proprietary)

7 CONCLUSIONS

The structural adequacy of the STP Unit 3 dryer is based on [ ]a,c The approach to qualify the STP Unit 3 dryer using the guidance of RG 1.20 Revision 3 (Reference 7-1) is based on the following.

- Operating Experience

  [ ]a,c

- Design Modifications to Avoid Acoustic Resonance

  [ ]a,c

- Instrumentation During Startup

  [ ]a,c

- Structural Evaluation Using RJ-ABWR Startup Data

  [ ]a,c

In summary it can be stated that:

- The ABWR design is an evolutionary design that has incorporated design changes and improvements based on operational experience of previous generations of BWR designs.
- RJ-ABWR has undergone an extensive preoperational and power testing and a thorough inspection program during startup without showing any damage to the dryer.
- RJ-ABWR and J-ABWR have accumulated over 12 years of operation without any indication of damage to the dryers as shown by the results of inspections described in Reference 7-2.
- RJ-ABWR and J-ABWR have never undergone any repairs to the dryers.
- STP Units 3 and 4 dryers are essentially identical to RJ-ABWR and J-ABWR in both structural configuration as well as operational parameters.
- Acoustic resonance has been eliminated [ ]^{a,c}
- The STP Unit 3 dryer will undergo a CVAP that involves a power ascension plan to hold the power level at [ ]^{a,c} to collect [ ]^{a,c} to allow development of limit curves for power levels up to 100% power in discrete steps.

This report concludes that the STP Unit 3 dryer would meet the cyclic stress requirements and perform without degradation during power operation.

7.1 REFERENCES FOR SECTION 7

7-1 U.S. NRC Regulatory Guide 1.20, Rev. 3, "Comprehensive Vibration Assessment Program for Reactor Internals during Preoperational and Initial Startup Testing," March 2007.

7-2 Westinghouse Report, WCAP-17369-P, "ABWR Dryer Operating Experience for STP Units 3 and 4," February 2011. (Proprietary)

This page left intentionally blank.